KSCE Journal of Civil Engineering (2021) 25(4):1353-1368
DOI 10.1007/s12205-021-0632-6

pISSN 1226-7988, eISSN 1976-3808
www.springer.com/12205

Structural Engineering

Theoretical Study on the Influence of Welding Collar on the Shear Behavior of Stud Shear Connectors

Yulin Zhan[a,b], **Siji Lu**[a], **Yuanbiao Zheng**[c], **Haijun Jiang**[d], **and Shaohui Xiong**[c]

[a]*Dept. of Bridge Engineering, Southwest Jiaotong University, Chengdu 610031, China*
[b]*Institute of Civil Engineering Materials, Southwest Jiaotong University, Chengdu 610031, China*
[c]*Ningbo Communications Planning Institute Co., Ltd, Ningbo 315100, China*
[d]*Qingdao Municipal Engineering Design Research Institute, Qingdao 266071, China*

ARTICLE HISTORY

Received 10 April 2020
Revised 1st 5 August 2020
Revised 2nd 24 September 2020
Accepted 27 November 2020
Published Online 12 February 2021

KEYWORDS

Shear stud
Welding collar
Push-out test
Finite element analysis
Structural parameters

ABSTRACT

Arc stud welding will melt the root of the stud to form a welding collar. For the purpose of exploring the influence of welding collar, numerical method is adopted for the theoretical analysis on shear resistance of the stud under several groups of different welding collar parameters. Firstly, the shear resistance between whether the headed studs considering the welding collars or not is compared. Then, the radius and height parameters of welding collar are changed. Finally, the increment ratio of bearing capacity by welding collars with the same height-diameter ratio is taken into consideration. Experimental data from three push-out test are adopted to validate the accuracy of the numerical method. The results show that the welding collar changes the yield area at the bottom of the stud. The height parameter has less influence than the radius. Under the condition that welding collars have the same height-diameter ratio, the improvement of shear resistance with different diameters roughly converges to 7.28%. The formulas of various countries show that at the height-diameter ratio of 0.25, the average value of bearing capacity of welding collar in various specification approach 7.1% of formula value.

1. Introduction

In recent decades, due to the excellent mechanical properties of composite structures, steel-concrete composite beams have been widely used in buildings and bridges (Chung et al., 2016; He et al., 2017). The transmission of longitudinal shear force at the steel-concrete interface is mainly realized through shear connectors (Xu et al., 2014a; Han et al., 2017). Currently, studs have become the most commonly applied shear connectors with the best performance in comprehensive stress and workability (Pathirana et al., 2015). For the sake of studying the shear behavior of headed studs, researchers from various countries have studied many kinds of test methods, among which the most classic one is the push-out test (Hanswille et al., 2007; Luo et al., 2016). With the aid of push-out tests, many researchers have conducted extensive research on the mechanical behavior of headed stud. For instance, Viest (1956, 1960) are the first to find that the shear resistance of studs is controlled by the tensile yield strength of the stud material itself and the plasticity of concrete through the static push-out test of shear studs. Ranzi and Bradford (2007), Xue et al. (2008), Han et al. (2015), found that the parameters affecting the performance of headed stud mainly include the diameter, height and tensile strength of stud, type of the slab, temperature gradient and reinforcement structure of concrete. Johnson et al. (1969) and Ollgaard and Slutter (1971) and others proposed the calculation model and formula of stud bearing capacity. In addition, the studs with large diameter has also been widely investigated. Hirama et al. (2017) collected and sorted out a great number of test results and evaluated the failure mode and shear resistance of studs under different conditions. Wang et al. (2018) found that Ultra-High Performance Concrete (UHPC) can give full play to the performance of large diameter studs, and put forward an empirical formula to evaluate the load-slip curve of studs according to the test results. Apart from push-out tests, a large number of finite element modelling techniques have been developed to expand the research scope. Finite element modelling

CORRESPONDENCE Yulin Zhan yulinzhan@home.swjtu.edu.cn Dept. of Bridge Engineering, Southwest Jiaotong University, Chengdu 610031, China; Institute of Civil Engineering Materials, Southwest Jiaotong University, Chengdu 610031, China

technology can not only reduce the number of tests, provide details of internal failure of test specimens but also find key parameters that affect performance (Xu et al., 2014b; Classen et al., 2016). Lam and El-Lobody (2005) carried out numerical simulation of the push-out test with considered the nonlinearity of concrete and steel, and verified it according to the test results, proving the accuracy of the finite element modelling push-out test. Qi et al. (2017) studied the influence of the damage degree at different positions on the shear stiffness and bearing capacity of studs, and proposed a theoretical formula considering the initial damage. Guezouli and Lachal (2012) carried out numerical analysis and quantitatively studied the effect of friction coefficient on the push-out test of studs. Although numerous researchers have carried out experiments and theoretical analyses on headed stud, few people have studied the influence of welding collars produced during stud forming process on the bearing capacity of stud connectors. In the welding process of stud connectors, the special stud welding gun is combined with the electric arc welding technology (ANSI/AWS C5.4-93, 1993) to melt, cool and form the stud root for the forming of welding collar (Chambers, 2001). The forming of welding collar will leads to the increase of the cross-sectional area at the root of stud. However, studies of its influence on the mechanical properties of the stud is limited so far. Only a few researchers have made some exploratory attempts. For example, Hiragi and Matsui (1998) optimized the welding ferrule and welding method to improve the fatigue strength of stud connectors. Higashiyama et al. (2014) improved the ferrules of stud welding to enhance the fatigue duration of headed stud and determine the fatigue strength of the improved headed stud under different concrete strengths.

Therefore, this study investigated the shear behavior of the headed studs with consideration to welding collar. A push-out test of stud shear connector is designed and compared with the theoretical analysis. On the basis of verifying the finite element model, tests are performed to probe into the influence of welding collars with different structural parameters of the welding collar on the shear behavior of headed stud, and the numerical analysis results is compared with the prediction results of different countries' formulas, and some useful conclusions are obtained.

2. Push-Out Test

2.1 Design of Test Specimens

Push-out test is one of the most representative test methods, in which test specimens are generally made of two concrete slabs and one steel beam (Fig. 1). The size and test method of the specimen conform to the Eurocode 4, i.e., Design of composite steel and concrete structures Part-1: general rules and rules for building (EC4, 2004), which is widely applied in China and the West.

The push-out test specimens are made of C60 concrete slabs, Q235 H-shaped steels and stud shear connectors. The specification

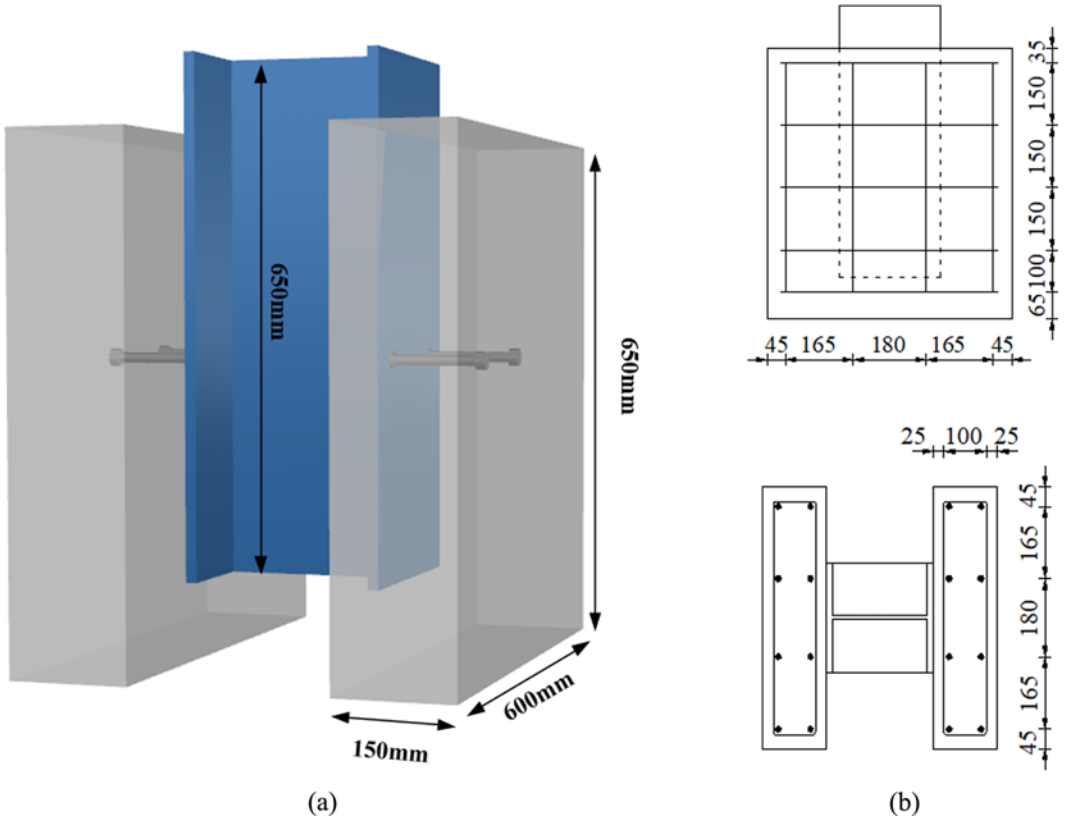

Fig. 1. Standard Specimen for the Stud Push-Out Test: (a) Three Dimensional Views of Specimen, (b) Details of Specimen (unit: mm)

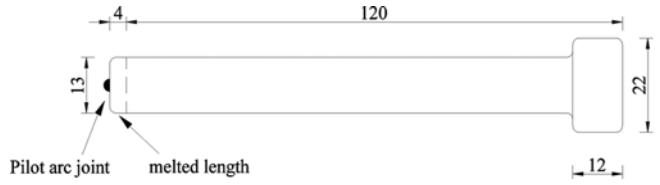

Fig. 2. Dimensions of the Cheese Head Stud (mm)

of stud shear connector is Φ13 mm × 120 mm and its material is Q235 steels. The melted length of stud is 4 mm, whose end is equipped with pilot arc joint. The specific dimensions are shown in the Fig. 2. The measured material strength of steels is shown in Table 1. The average elastic modulus of tested C60 concrete is 31.5 GPa and the average Poisson's ratio is 0.18. The mix design for C60 concrete is given in Table 2.

According to (CECS226-2007, 2005), stud shear connectors are welded on steel beams by drawn arc stud welding technology. As illustrated by Hildebrand and Soltanzadeh (2014), The procedure of drawn arc stud welding is demonstrated as Fig. 3. The welding procedure is as following: 1) Preparation: prepared the stud and temperoried auxiliaries, the stud is placed against the workpiece. 2) Pilot arc: The stud is lifted off while current is flowing, thus creating an arc. 3) Welding: The arc melts the surface of the stud and workpiece. 4) Pressurizing: The stud is plunged into the weld pool. 5) Power off: A cross-sectional joint is achieved. 6) Cooling: The welding is cooling and the welding collar is formed.

Table 2. Mix Design for C60 Concrete

Materials	Quantity
Cement (kg/m^3)	480
Water (kg/m^3)	146
Fine aggregate (kg/m^3)	605
Coarse aggregate (kg/m^3)	1,075
Fly ash (kg/m^3)	50
Admixture (kg/m^3)	12.4
Water/cementitious materials	0.30

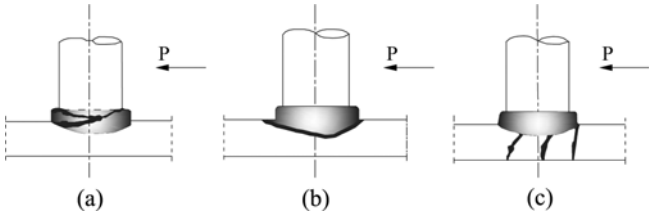

Fig. 4. Failure Models of Shear Studs: (a) Model A, (b) Model B, (c) Model C

From the previous research, the failure models of headed studs are concluded as three types shown as Fig. 4. In Model A, crack is initially generated at the shank of the stud and the successive crack penetrated the welding collar and the shank respectively. In Model B, crack is initially generated at the bottom of the welding collar and courses the welding affected

Table 1. Test Results of Steel Mechanical Properties

Projects	Yield strength (MPa)	Ultimate strength (MPa)	Yield ratio	Elastic modulus (GPa)	Poisson's ratio
Steel beam	370.4	513.3	0.72	202.3	0.28
Stud	263.1	499.8	0.53	203.2	0.27
Stirrup	433.5	565.7	0.77	193.2	0.27

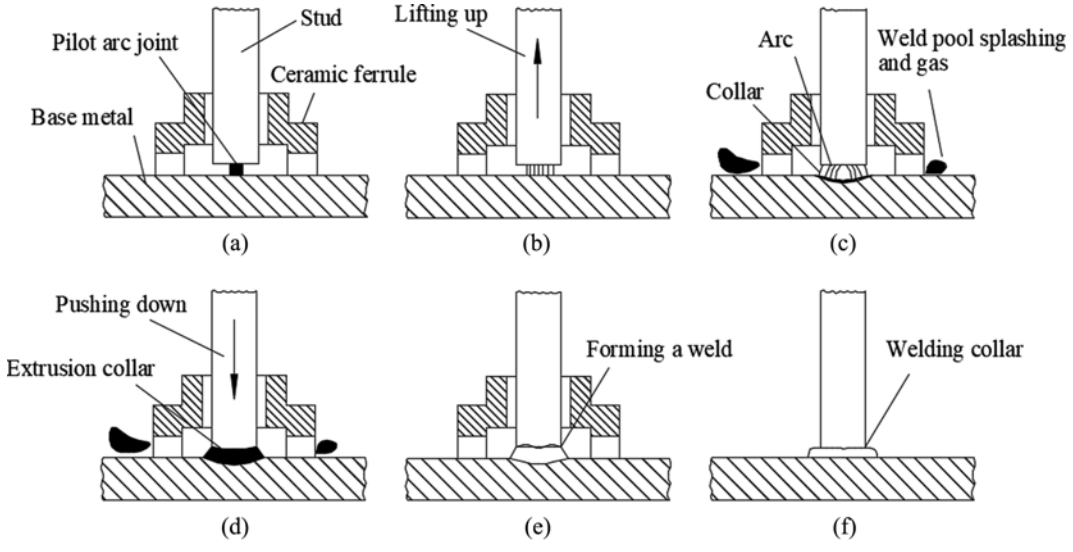

Fig. 3. The Process of Drawn Arc Stud Welding: (a) Preparation, (b) Pilot Arc, (c) Welding, (d) Pressurizing, (e) Power Off, (f) Cooling

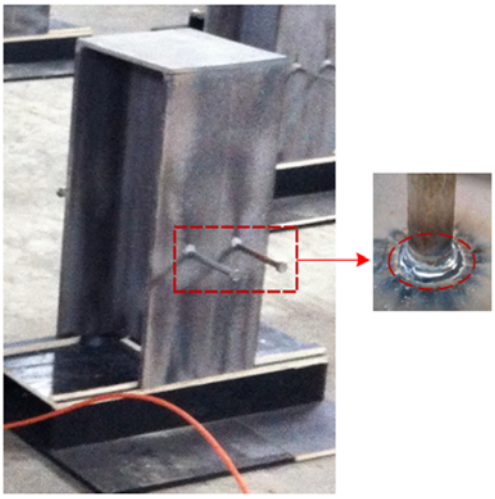

Fig. 5. Finished Welding Products of Steel Beams and Stud Connectors

Fig. 6. Finished Products of the Push-Out Test Specimens

area in the flange material. In Model C, crack is initially generated at the bottom of the welding collar and successive crack forms either directly through the flange or first alongside the welding affected area and then through the flange. However, the influence by the welding collar to the shear capacity was not yet be studied.

Steel beam are assembled by welding of steel plates, and a steel plate for load application is welded on the top of the steel beam in accordance with the Code for Welding of Steel Structures (GB50661-2011, 2011). The steel beam is made of HW250 × 250 × 9 × 14 steel, and the thickness of steel plate in the loading area at the top is 12 mm. According to the Technical Specification for Welding of Stud (CECS226-2007, 2005), the arc stud welding technology is applied to weld the headed studs on steel beam. The process of welding is displayed at Fig. 3. The welding collar formed after the root of the stud melts is as shown in Fig. 5, and the physical photos of the processed test specimens are shown in Fig. 6.

2.2 Test Program

The test loading is carried out by a press. For uniform load distribution, a steel ingot is placed on the top of the test specimen, and the bottom of the test specimen is leveled with gaskets. The test set-up and instrumentation is shown in Fig. 7. The process of loading should conform to the following requirements:

1. Preloading. The first step is to preload to no more than 40% of the expected ultimate loading.
2. Step loading. Twenty percent (20%) of the ultimate loading is set as the load increment before the steel yield, and the load increment is reduced after the yield stage.

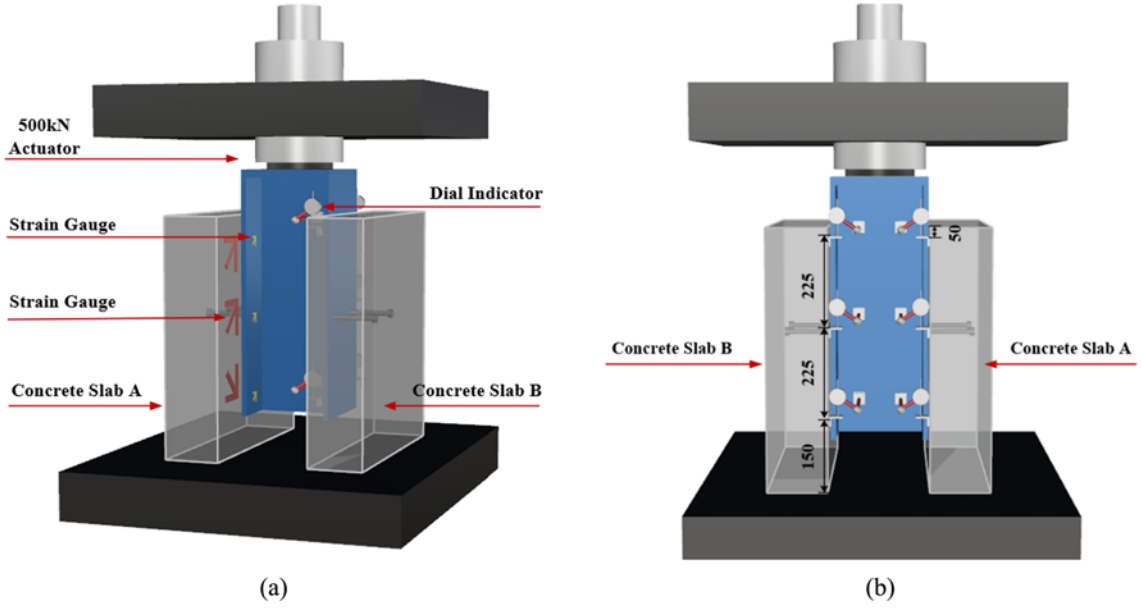

Fig. 7. Test Set-Up and Instrumentation: (a) Front View, (b) Back View

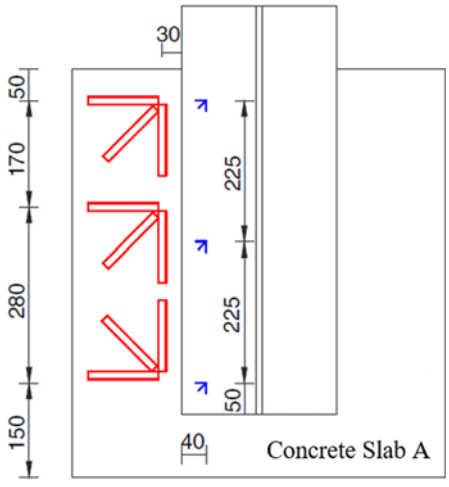

Fig. 8. Strain Gauge Layout (mm)

Fig. 9. Test Loading

When the load-slip curve approaches the horizontal section, displacement controlled loading is adopted.

3. Each stage of loading shall be kept stable for 5 minutes, during which the data can be read and recorded.
4. The specimen shall be unloaded after it is damaged.

The results of push-out tests shall include the concrete slab strain, steel beam strain, load-slip curves and the failure modes of specimens. The relative slip between the steel surface and concrete surface is caught through a dial indicator (to the precision of 0.01 mm), and eight dial indicators are installed from top to bottom of the steel-concrete interface. Among them, the measuring points 1 and 2 are set on the concrete slab B opposite to the concrete strain gauge, and the measuring points 3 to 8 are respectively set on the other sides of the concrete slab A and B. The positions of specific measuring points are shown in Fig. 7.

The strain is obtained by measuring strain gauges pasted on the surfaces of steel beams and concrete slabs. The strain gauges are arranged in the triaxial directions with angles of 45°as shown in Fig. 8. The test loading photos are shown in Fig. 9.

3. Finite Element Modelling

3.1 Finite Element Model

To compare and analyze the test results, the corresponding finite element model was established by the software ABAQUS. For the symmetry of structure, the structure is simplified into a model structure with size of a quarter of the original as shown in Fig. 10. All nodes of the concrete slab in the opposite direction of loading are restricted from moving in the Z direction to resist the compression load and symmetric constraints are imposed on the symmetry planes. The linear reduced integration hexahedral element C3D8 is adopted for the stud and steel beam, T3D2 element is used for reinforcement, while the elements C3D8 and C3D4 are employed for the concrete. When meshing components, attention should be paid to areas with complex stress such as the interface between concrete slab and stud, and the interface between stud and steel beam. Meanwhile, the mesh should be refined. In other areas, the mesh size can be appropriately increased. The stud is divided into 12 elements in Y direction and 20 elements in circumferential direction .The overall seed size of concrete slab is set as 50 mm and the local seed size is about 8 mm to improve the calculation speed when the accuracy can be ensured.The displacement loading method is adopted in the model. Before the relative slip between steel and concrete surfaces, The shear force of the structure is borne by the cohesive force of the interface; and when the slip occurs, cohesive force will be converted into friction force and the shear force on the structure is shared by the stud shear connector and friction force. In addition, friction contact is introduced into the finite element model. Under the regulation of the AASHTO LRFD Bridge Design Specification, the friction coefficient is set to be 0.7, so as to more accurately simulate the influence of friction force in the early stage of the actual test. The contact between the surfaces of concrete and studs is defined as hard. When the contact pressure becomes zero or negative, the two contact surfaces will be separated from each other. The bond behavior is adopted for the contact between stud and steel beam. As the load continues to

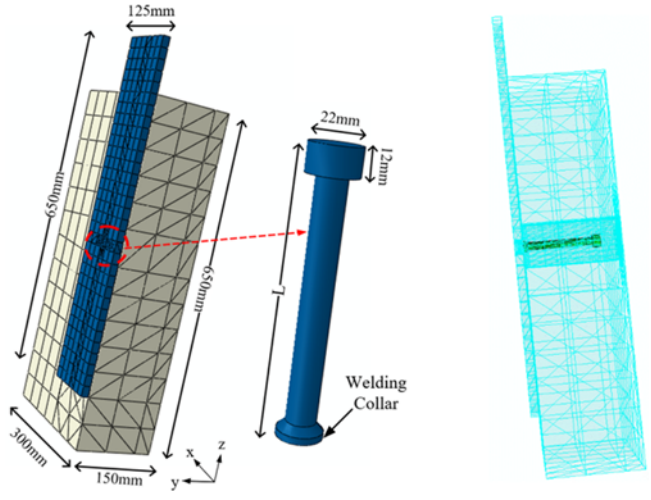

Fig. 10. Finite Element Analysis Model

increase, the steel surface will be separated from the concrete surface (Lam and EI-Lobody, 2005) and then friction force will thus disappear. At this time, the test specimens will provide the interface shear resistance through the shear connectors.

3.2 Constitutive Relation of Materials

3.2.1 Constitutive Relation of Concrete

In this paper, Hongnestad curve (Hognestad, 1951) is adopted for the stress-strain curve of concrete under uniaxial compression, which is divided into a ascending segment of quadratic parabola and a descending segment of oblique straight line. The expression is shown in Eq. (1), wherein the stress-strain curve of concrete is shown in the Fig. 11. E_0 in the Fig. 11 refers to the initial elastic modulus.

$$\sigma=\begin{cases}\sigma_0\left[2\left(\dfrac{\varepsilon}{\varepsilon_0}\right)-\left(\dfrac{\varepsilon}{\varepsilon_0}\right)^2\right] & \varepsilon\le\varepsilon_0\\ \sigma_0\left[1-0.15\dfrac{\varepsilon-\varepsilon_0}{\varepsilon_u-\varepsilon_0}\right] & \varepsilon_0<\varepsilon<\varepsilon_u\end{cases} \tag{1}$$

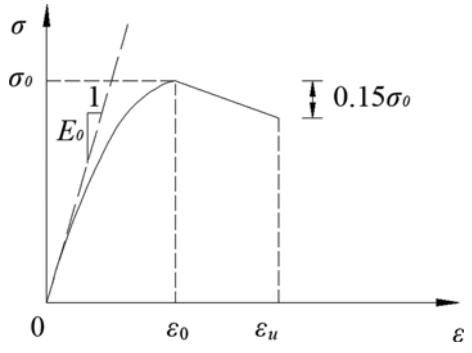

Fig. 11. Stress-Strain Relation of Concrete

In the formula, ε_0 refers to compressive strain and $\varepsilon_0 = 0.002$ is preferable; ε_u means ultimate compressive strain and $\varepsilon_u = 0.0038$ is desirable; σ_0 is peak stress, $\sigma_0 = 0.85\ f_c'$ is advisable; $\sigma_0 = 62$ MPa and $E_0 = 31{,}530$ MPa.

3.2.2 Constitutive Relation of Steel

The Mises yield criterion is adopted for steels in this paper. The stress-strain curve of steel is simplified as shown in the Fig. 12. The elastic stage and the strengthening stage are linear. The elastic-plastic stage is a curve. With the increase of stress, the tangent modulus of steel gradually reduces to zero in the plastic stage and then enters the strengthening stage. The plastic stage and secondary plastic flow are straight lines. The stud failure is simulated by defining a descending segment.

4. Results Analysis and Comparison

4.1 Model Verification

The accuracy of the numerical analysis model is confirmed by quoting the data of Lam's ordinary stud push out test and Lam's specimen parameters are presented in Table 3 (Lam and El-Lobody, 2005). The calculated value of the numerical analysis model is compared with the test value of the specimen. As shown in Figs. 13 and 14, when the influence of the stud welding collar is taken into consideration, the calculated value data of the finite element model fit well the test value data and the maximum error of ultimate bearing capacity is 4.5%. When the slip is 2 mm, the average error between the test value and the calculated value of the shear load is 11.3%, thus the test value of ultimate bearing capacity basically matches the calculated one. When the influence of the stud welding collar is not taken into consideration, the calculated results are quite different from the test values, which indicates the necessity of considering welding collar.

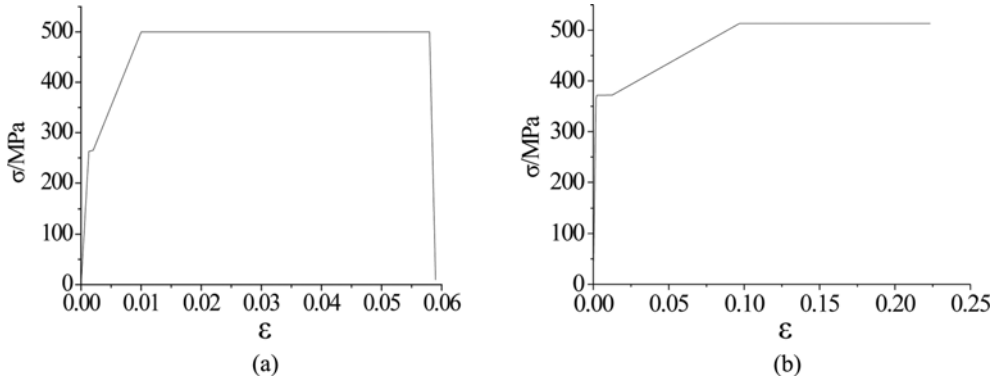

Fig. 12. Constitutive Relation Curve of Steel Plate and Stud: (a) Stud, (b) Steel Plate

Table 3. Specimens for Push-Out Tests of Lam's Research

Test specimens	Diameter of headed stud (mm)	Height of headed stud (mm)	Ultimate strength of stud (MPa)	Elastic modulus of stud (GPa)	Concrete strength (MPa)	Elastic modulus of concrete (GPa)
SP3	19	100	470.8	200	30	22.82
SP4	19	100	470.8	200	35	24.65

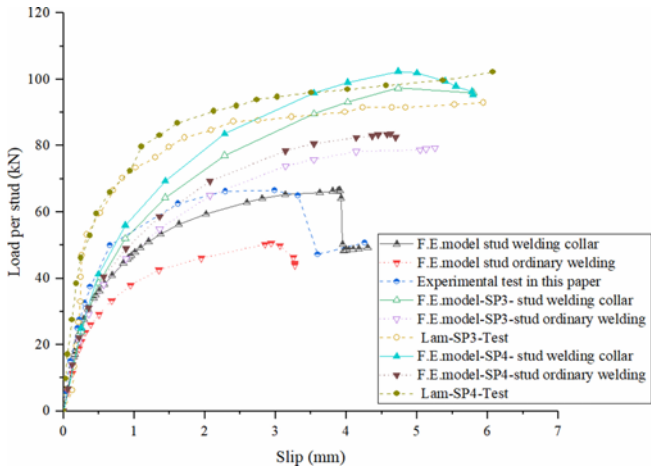

Fig. 13. Load-Slip Curves

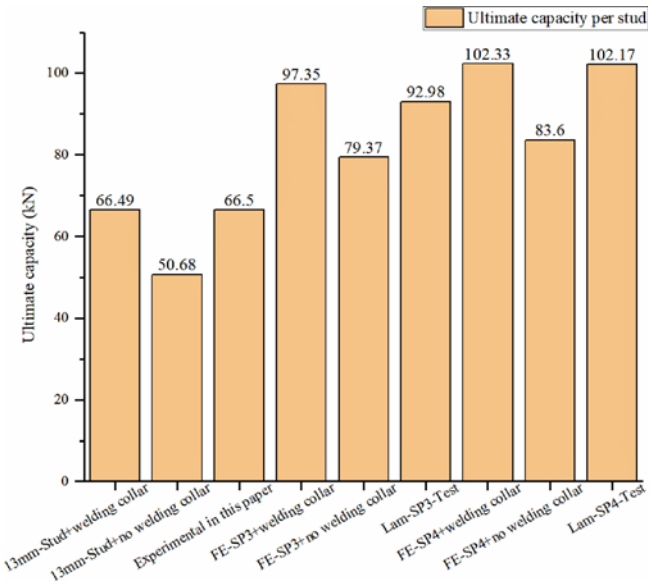

Fig. 14. Comparison of Ultimate Capacity of Different Specimens

4.2 Failure Modes of Specimens

When the push-out test specimen is damaged, the failure mode is shown as the shearing of stud, since the concrete strength of the specimen is high. After the specimen is damaged and the stud is found sheared by peeling off the components, the welding collar and the root of stud will remain on the steel beam, which increases the roughness of the interface. Besides, the contact part of the concrete slab with stud tends to be "drilled", and there are still scratches left by the welding collar and the root of the stud across the contact part of the concrete. The failure mode of the specimen is as shown in the Fig. 15. Both theoretical and experimental results show that when the specimen is damaged, the stud stress is in a high stress state but the welding collar has not been sheared. Meanwhile, the stress level of concrete connected with the shear connector is high, and the concrete in contact with the stud is seriously damaged.

Under the state of ultimate bearing capacity, the stress distribution of concrete is shown in Fig. 16. At this time, part of the concrete at the root of the stud gains the ultimate strength, while the height of concrete reaches nearly 150 mm in the vertical direction of the area under stud pressure. A cross-section diagram can be obtained through cutting through the concrete slab from the middle, as shown at the right of Fig. 16. It can be seen that the depth of influence of the stud on the concrete slab reaches 60 mm. The stress distribution diagram of the stud under the state of ultimate bearing capacity is shown in the stress diagram in Fig. 17. At this time, yield strength of the stud reaches the ultimate, and the stress range of the stud reaches 85 mm in the lengthwise direction. As can

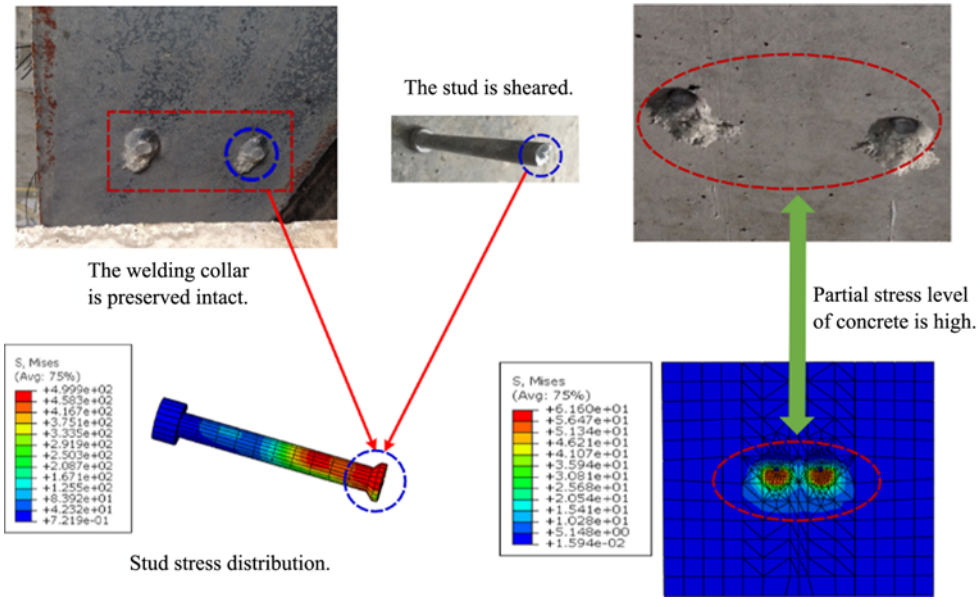

Fig. 15. Failure Modes of Push-Out Test Specimens (MPa)

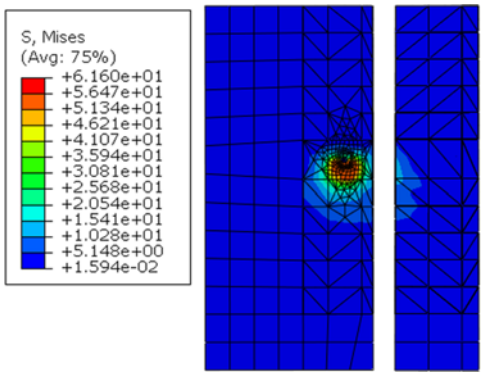

Fig. 16. Stress Distribution of Concrete Slab (MPa)

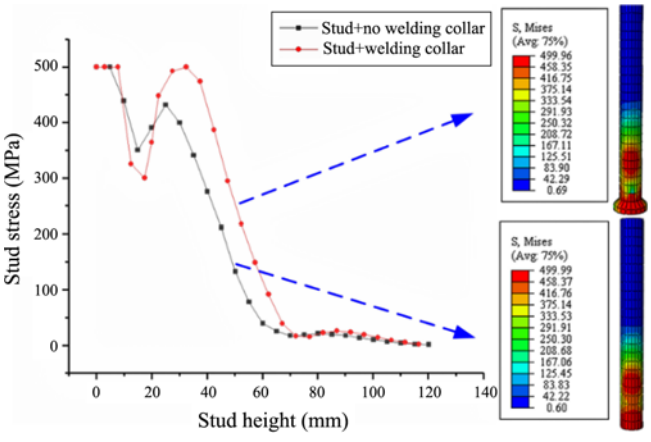

Fig. 17. Stress Distribution of Studs (MPa)

be seen from the Fig. 17, the main load-bearing section of the stud is near the root, while the stress on the head of the stud is relatively small. Therefore, in the subsequent modeling calculation, the solid model of the stud is simplified, and the stud is simulated by using a cylinder with studs of the same diameter at the head and root. The comparison of stud stress state is shown in Fig. 17. In the picture, the stress is distributed non-linearly along the stud height direction, and the stress level at the root of the stud is relatively high. Obviously, the stress distribution of stud with welding collar is different from that of stud without welding collar.

5. Parameter Analysis

5.1 Parameter Design

For the sake of studying the influence of welding collar on the shear resistance of stud, 18 sets of finite element numerical analysis models are set up with reference to the Welding — Studs and ceramic ferrules for arc stud welding (ISO 13918, 2017), and the relevant parameters are shown in Table 4. They are divided into 3 groups. Group 1: comparing the influence of stud and stud + welding collar on mechanical properties; Group 2: changing the radius, height and volume of stud welding collar; Group 3: modifying the stud diameter under the condition that the height-diameter ratios of welding collars are same, and investigate the contribution of the welding collars to shear capacity. To facilitate the description of the influence of the welding collar, the welding collar is assumed to be idealized in parameters. The assumed welding collar size is shown in Fig. 18.

5.2 Influence of Studs with and without Welding Collars

When we keep the size of the welding collar unchanged, and uniformly adopt $h_1 = 3.5$ mm, $h_2 = 3$ mm, $h_3 = 3.5$ mm, four load-

Table 4. Setting of Calculation Parameters

Group	No.	Content	D (mm)	H (mm)	h_1 (mm)	h_2 (mm)	h_3 (mm)	Ultimate capacity (kN)
Group 1	C1	Stud + No welding collar	13	120	0	0	0	50.68
	C1’	Stud + Welding collar	13	120	3.5	3	3.5	66.50
	C2	Stud + No welding collar	16	120	0	0	0	75.15
	C2’	Stud + Welding collar	16	120	3.5	3	3.5	88.06
	C3	Stud + No welding collar	19	120	0	0	0	104.14
	C3’	Stud + Welding collar	19	120	3.5	3	3.5	111.17
	C4	Stud + No welding collar	22	120	0	0	0	140.02
	C4’	Stud + Welding collar	22	120	3.5	3	3.5	138.22
Group 2	C5	Radius of welding collars: $h_1 = 2$ mm	19	120	2	3	3.5	92.62
	C6	Radius of welding collars: $h_1 = 2.5$ mm	19	120	2.5	3	3.5	95.52
	C7	Radius of welding collars: $h_1 = 3$ mm	19	120	3	3	3.5	101.26
	C8	Height of welding collars: 50% of h_2, 50% of h_3	19	120	3.5	1.5	1.75	100.16
	C9	Height of welding collars: 80% of h_2, 80% of h_3	19	120	3.5	2.4	2.8	107.63
	C10	Welding collars with equal volume	19	120	2.5	5.4	2.5	107.53
Group 3	C11	D = 13 mm, $h_1 = 2.5$ mm	13	120	2.5	2	2.5	54.46
	C12	D = 16 mm, $h_1 = 3$ mm	16	120	3	2.5	3	80.80
	C13	D = 19 mm, $h_1 = 3.5$ mm	19	120	3.5	3	3.5	111.17
	C14	D = 22 mm, $h_1 = 4$ mm	22	120	4	3.5	4	148.43

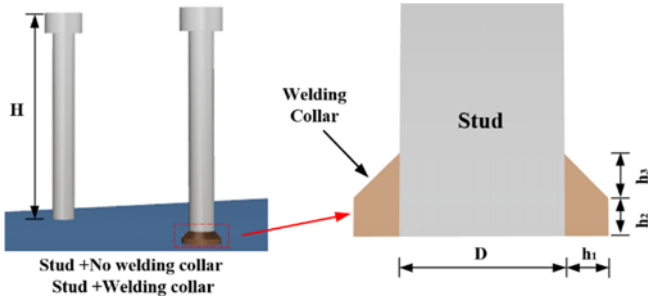

Fig. 18. Parameters of Welding Collar Formed by Stud Welding

slip curves can be obtained when the stud diameters are 13 mm, 16 mm, 19 mm and 22 mm, as shown in Fig. 19. It can be obtained from Fig. 19 that the influence of the welding collar on the load-slip curve at the initial loading stage can be almost ignored. Whereas, as the growth of the load, the contribution of welding collar on the mechanical behavior becomes greater, which can be manifested by the increase of peak load and the enhancement of rigidity.

Because the slip of 2 mm produces about 90% of the ultimate shear resistence, the load (V_0. 002) corresponding to 2 mm slip and the peak load (V_max) are selected to quantitatively analyze, and the influence of relative volume of welded collar on the shear resistence of stud are investigated. The formula is as follows:

$$\alpha_1 = \frac{Vol_{\_ring}}{Vol_{\_stud}}, \tag{2}$$

$$Vol_{\_stud} = \frac{\pi D^2}{4}\left(h_2 + \frac{h_3}{2}\right), \tag{3}$$

$$Vol_{\_ring} = \left(h_1 h_2 + \frac{h_1 h_3}{2}\right)\pi(D + h_1), \tag{4}$$

where α_1 – influence parameters; $Vol_{\_stud}$ – volume of studs

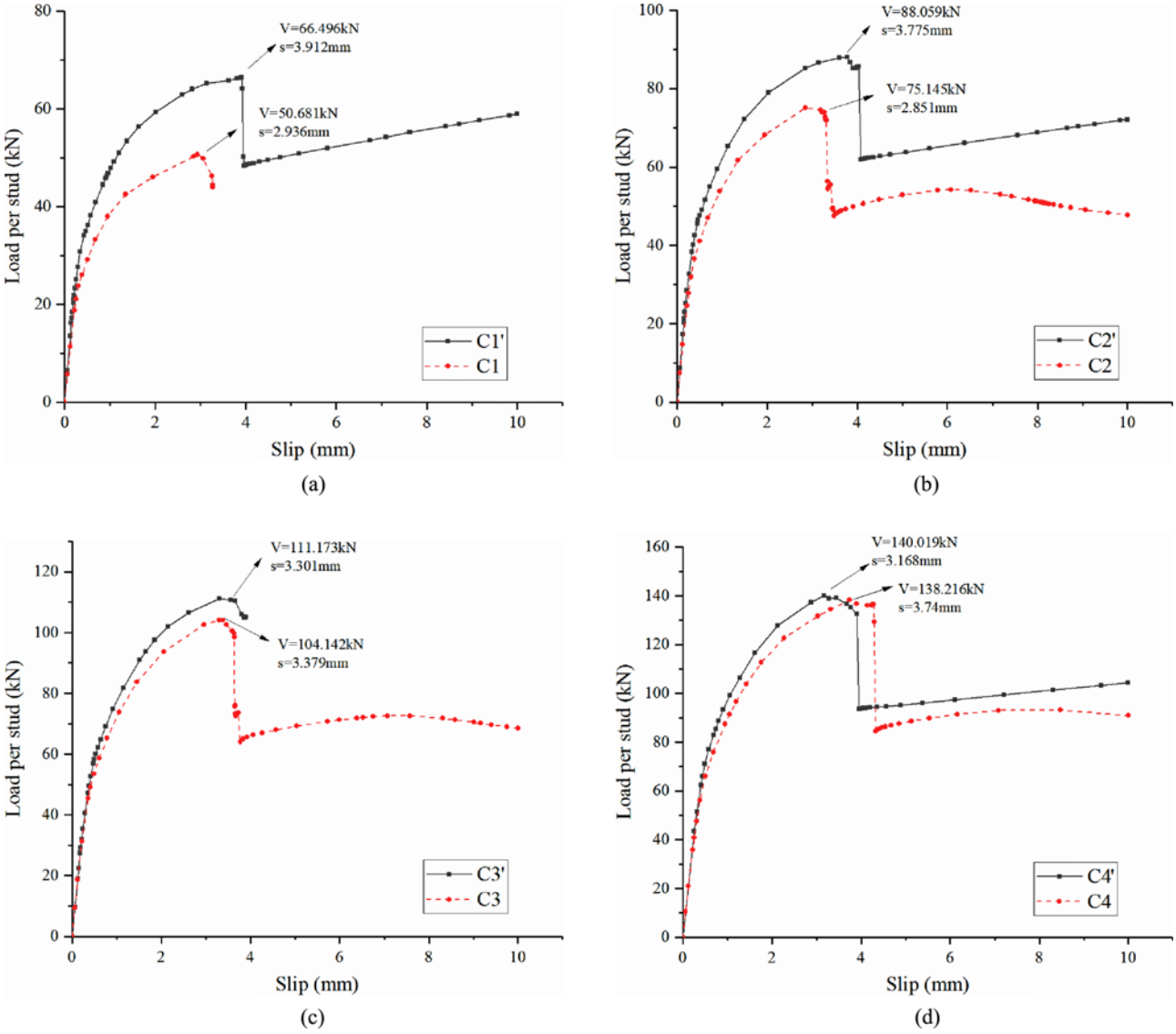

Fig. 19. Load-Slip Curves for Different Stud Diameters: (a) D = 13 mm, (b) D = 16 mm, (c) D = 19 mm, (d) D = 22 mm

Table 5. Results of the Influence of Studs with and without Welding Collars on the Bearing Capacity

No.	Vol_{-ring} (mm^3)	Vol_{-stud} (mm^3)	α_1	V-max (kN)	Percentage	V_0.002 (kN)	Percentage
C1	0	0	—	50.68	—	46.30	—
C1'	861.79	630.48	1.37	66.50	31%	59.27	28%
C2	0	0	—	75.15	—	68.60	—
C2'	1018.47	955.04	1.07	88.06	17%	78.65	15%
C3	0	0	—	104.14	—	92.73	—
C3'	1175.16	1346.76	0.87	111.17	7%	99.70	8%
C4	0	0	—	138.22	—	117.33	—
C4'	1331.84	1805.63	0.74	140.02	1%	123.63	5%

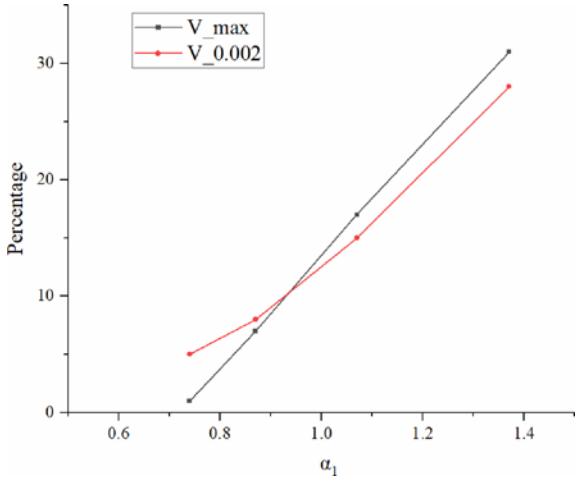

Fig. 20. Curve of the Relation between α_1 and Bearing Capacity

(mm^3) with the same height; Vol_{-ring} – volume of welding collars (mm^3) with the same height.

Whether the welding collar has an effect on the shear resistance of stud is shown in Table 5 and Fig. 20, from which it is clear that the shear resistance of stud is enhanced with the increase of α_1 and the relationship between α_1 and the increment of the bearing capacity is almost linear. When the diameter of stud increases, the relative volume ratio of welding collar decreases due to the constant volume of welding collar, which leads to the decrease of the contribution of welding ring to bearing capacity.

Figure 21 shows the stress distribution of studs with different diameters along the height direction. It can be concluded that stress starkly concentrated at the root of the stud. Along the height direction, the stud stress first decreases and then increases, and a higher stress level emerges in the middle. Finally, stress gradually decreases from the middle to the top. For the stud with welding collar, the yield area at the bottom of the stud is larger and the effective shear resistance area is also larger than those without welding collar.

For the sake of studying the influence of welding collar on the stress distribution, the integral results of stress along the height direction are shown in Table 6. In this table, it can be seen that compared with the stud without welding collar, the integral area of the stud with welding collar has increased correspondingly, which indicates that the welding collar has enhanced the energy dissipation capacity. With the increase of stud diameter, the increment of welding collar's energy dissipation area decreases continuously, which reflects that as the growth of the stud diameter, the energy dissipation capacity of welding collar relative to stud itself decreases, and the contribution ratio of welding collar to the bearing capacity also declines.

5.3 Influence of Welding Collar Parameters

Take the stud connector (diameter: 19 mm) with a welding collar as an example. The radius of the welding collar are adjusted to 2 mm, 2.5 mm and 3 mm respectively, and the corresponding load-slip curves of different radii are calculated and drawn as shown in Fig. 22. According to the Fig. 22, It can be concluded that the radius of the welding collar has little influence on the

Table 6. Integral Results of Stud Stress Distribution

Model No.	Stud height (mm)	Integral area (N/mm)	Integral area increment%	Stud height (mm)	Integral area (N/mm)	Integral area increment%
C1	20	8,642.36	-5.09	120	20,014.75	21.28
C1'	20	8,223.75		120	24,274.87	
C2	20	8,122.98	5.24	120	25,368.29	5.14
C2'	20	8,572.26		120	26,672.17	
C3	20	7,511.12	14.18	120	26,780.42	5.12
C3'	20	8,751.96		120	28,151.15	
C4	20	7,260.72	18.81	120	29,955.52	0.32
C4'	20	8,942.77		120	30,050.09	

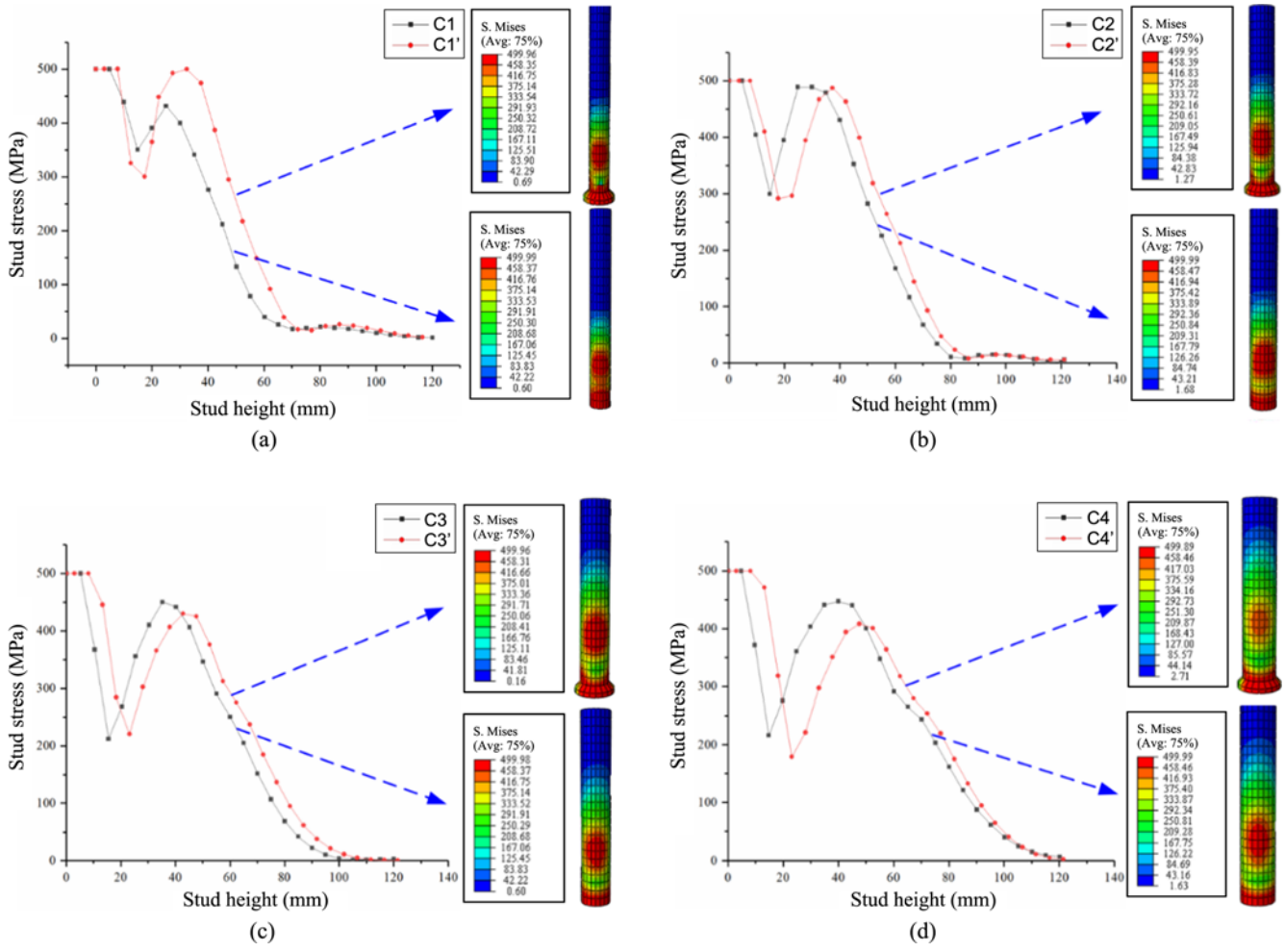

Fig. 21. Stress Distribution of Studs with Different Diameters: (a) D = 13 mm, (b) D = 16 mm, (c) D = 19 mm, (d) D = 22 mm

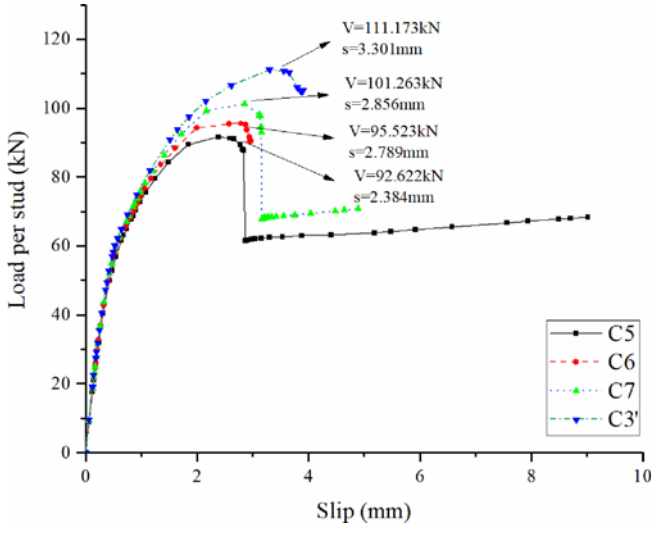

Fig. 22. Load-Slip Curves of Different Welding Collar Radii

load-slip curve at the initial stage of loading, and the difference occurs after the slip reaches 1.5 mm. The relation between ultimate bearing capacity and welding collar diameter is shown in Table 7, which shows that when the radius of welding collar increases from 2 mm to 2.5 mm, the corresponding ultimate bearing capacity increases by about 3.13%; when the radius rises from 2.5 mm to 3 mm, by about 5.67%; when the radius from 3 mm to 3.5 mm, by about 9.77%. There is no denying that the shear resistance of stud increased with the rise of the welding collar radius. However, the increment was not proportional, and the growth rate is increasing.

Table 7. Ultimate Bearing Capacity of Stud Shear Connectors with Different Welding Collar Radii

Model No.	h_l/mm	Slip/mm	Maximum bearing capacity (kN)	Percentage of increment in bearing capacity (%)
C5	2.0	2.94	92.62	—
C6	2.5	2.79	95.52	3.13
C7	3.0	2.85	101.26	5.67
C3'	3.5	3.30	111.17	9.77

With the stud connector (diameter: 19 mm) with welding collar as the benchmark, the height of the welding collar is

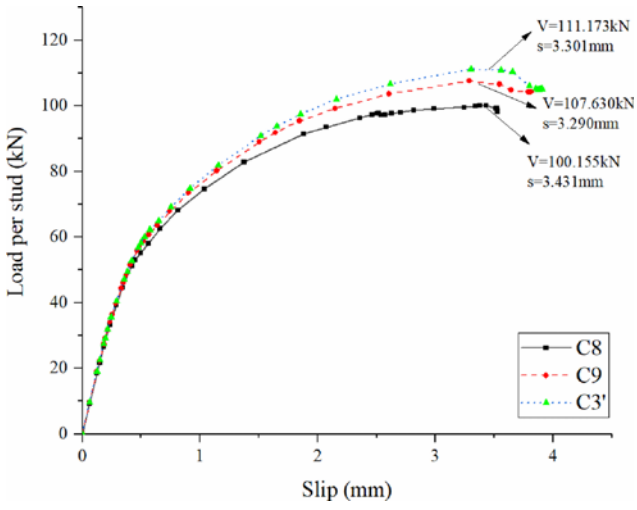

Fig. 23. Load-Slip Curves of Different Welding Collar Heights

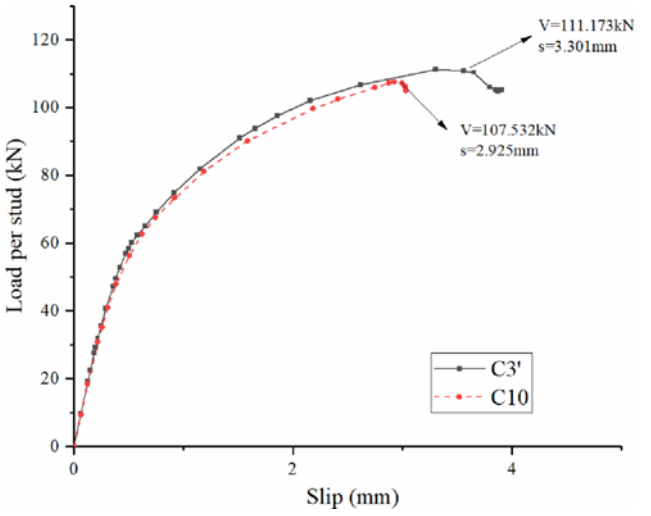

Fig. 24. Load-slip Curves of Welding Collars with Equal Volume but Different Radii

Table 8. Ultimate Bearing Capacity of Stud Shear Connectors with Different Welding Collar Heights

Model No.	Slip/mm	Maximum bearing capacity/kN	Percentage of increment in bearing capacity %
C8	3.43	100.16	7.46%
C9	3.29	107.63	
C3'	3.30	111.17	3.29%

Table 9. Ultimate Bearing Capacity of Stud Shear Connectors with Welding Collars with Different Radii and Equal Welding Collar Volume

Model No.	slip/mm	Maximum bearing capacity/kN	Percentage of increment in bearing capacity %
C10	2.93	107.53	3.39%
C3'	3.30	111.17	

adjusted to 80% and 50% of the original size respectively, and a load-slip curve with regard to the influence of the welding collar height h_2 and h_3 on the ultimate bearing capacity can be obtained as shown in Fig. 23. it can see that when the load is small, the influence of the welding collar height on the load-slip curve is small, and when the load is large, the influence gradually becomes greater. The relation between the ultimate bearing capacity and the welding collar height is shown in Table 8. it can obtain from this table that when the height of the welding collar increases from 50% to 80% of the original dimension, the corresponding ultimate bearing capacity increases by about 7.46%; when the height rises from 80% to 100% of the original size, the corresponding shear resistance is enhanced by about 3.29%. There is no denying that the shear resistance of stud intensified with the increase of the height of welding collar, but the growth rate tends to slow down.

In respect to stud shear connectors (diameter: 19 mm) with welding collars, test specimens C10 and C3' with different welding collar radii but the same volume are selected, and the welding collar size h_1 is adjusted from 2.5 mm to 3.5 mm and h_2 is adjusted from 3 mm to 5.4 mm, so as to ensure that the welding collars of the two models are equal in volume. The calculated load-slip curve is shown in Fig. 24, and the comparison of different ultimate bearing capacities is shown in Table 9. It shows that the load-slip curve of welding collars with the same volume is basically similar, but the larger the radius is, the greater the contribution to shear resistance is.

5.4 Results of the Same Height-Diameter Ratio

To study the influence of welding collar on shear resistance under the condition that stud diameters is different, but height-diameter ratio of welding collars is the same, *i.e.* $(h_2 + h_3)/(D + h_1) = 0.25$, specimens with welding collars of different radii but equal height-diameter ratio are selected. Take the stud with diameter of 13 mm and welding collar with radius of 2.5 mm and height of 4.5 mm as an example. The welding collar dimensions with different diameters are converted. The results of ultimate bearing capacity and shear resistance corresponding to 2 mm slip

Table 10. Comparison between Ultimate Bearing Capacity of Studs and the Bearing Capacity Increment under 2 mm Slip under the Same Height-Diameter Ratio

No.	V_ max(kN)	Percentage (%)	V_0.002 (kN)	Percentage (%)
C1	50.68	7.46	46.30	12.20
C11	54.46		51.95	
C2	75.14	7.53	68.60	10.17
C12	80.80		75.58	
C3	104.14	6.75	92.73	7.51
C13	111.17		99.70	
C4	138.22	7.39	117.33	9.95
C14	148.43		129.01	

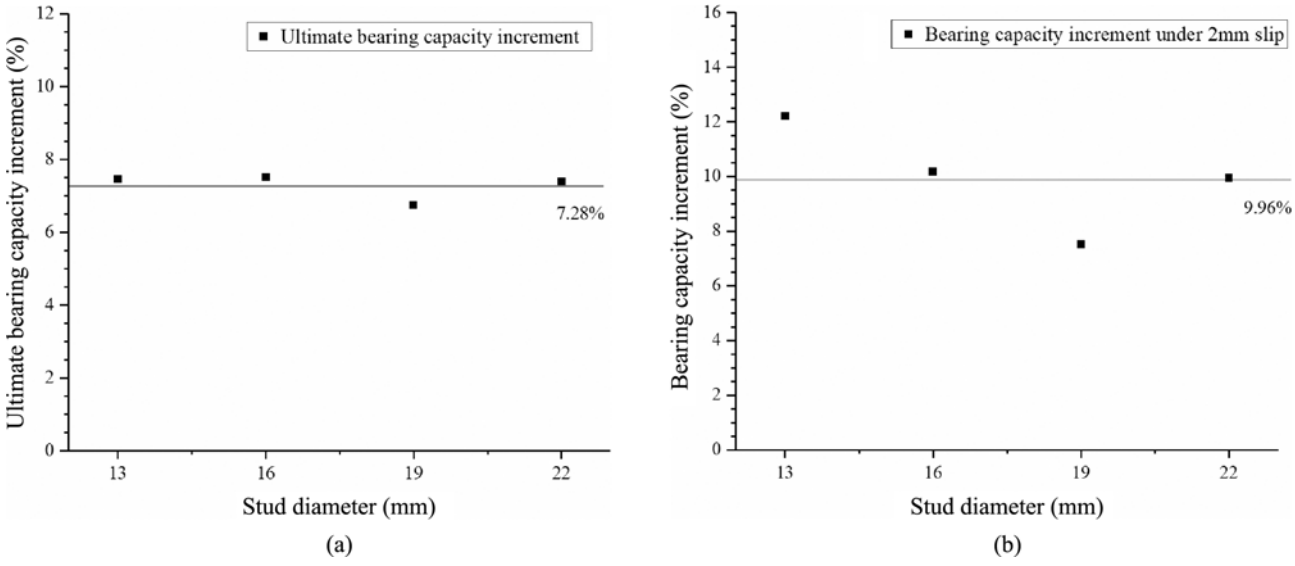

Fig. 25. Ultimate Bearing Capacity Increment of Studs with Different Diameters and Equal Height-Diameter Ratio: (a) Relation between Increment of V_ Max and Diameter, (b) Relation between Increment of V_0.002 and Diameter

are shown in Table 10 respectively, and the increment curve of shear resistance is shown in Fig. 25. It can be seen from the Fig. 25 that the peak load increment of studs with different diameters but the same height-diameter ratio is about 7.28%, and when the slip is equal to 2 mm, the corresponding increment of load (V_0.002) is about 9.96%. This shows that the contribution of the welding collar with the same height-diameter ratio to the bearing capacity converges to a constant value with approximately the same increment.

6. Study on Bearing Capacity Formula of Studs

To probe into the contribution of welding collar to the shear resistance, the shear resistances of the tests, FE model and different specifications are compared. After that, the stud specimen groups with the same height-diameter ratio are analyzed theoretically. Besides, the numerical analysis results of the ultimate bearing capacity are compared with the theoretical values of the existing standard formulas. For stud connectors, many different calculation formulas are adopted in specifications of various countries. The mainstream formulas in specifications are as follows:

The latest American Specification for Structural Steel Buildings ANSI/AISC 360-05, (ANSI/AISC, 2005) specifies the formula for the allowable bearing capacity of studs, as shown in Eq. (5):

$$Q_d = 0.5 A_s \sqrt{E_c f_c'} \le A_s f_u \,, \tag{5}$$

where Q_d – shear resistance of stud (N); A_s – cross-sectional area of stud (mm^2); E_c – elastic modulus of concrete (MPa); f_c' – compressive strength of concrete cylinder (MPa); f_u – ultimate tensile strength of stud (MPa).

A reduction factor of 0.7 is added to the right term in the bearing capacity formula proposed in the American LRFD bridge design specifications (AASHTO, 2012), as shown in Eq. (6):

$$V_u = 0.5 A_{st} \sqrt{f_c' E_c} \le 0.7 f_u A_{st} \,, \tag{6}$$

where V_u – shear resistance of stud (N); A_{st} – cross-sectional area of stud (mm^2);

The formula specified in Canadian Limit states design of steel structures (CAN/CSA-S16-01, 2005) specification is shown in Eq. (7):

$$V_u = 0.5 \phi_{sc} A_{st} \sqrt{f_c' E_c} \le \phi_{sc} f_u A_{st} \,, \tag{7}$$

where φ_{sc} – bearing capacity coefficient, with a value of 0.8

According to the analysis of tests and reliability research results of push-out tests by 75 entities in various countries around the world, the coefficients of the original formula in the EC4 is adjusted and the relatively small value among the results from the following formula of stud bearing capacity is obtained based on reliability analysis:

$$Q_d = 0.29 \alpha d^2 \sqrt{E_c f_{ck}} / \gamma_v \,, \tag{8}$$

$$Q_d = 0.8 A_s f_u / \gamma_v \,, \tag{9}$$

where α – influence coefficient of stud length ($\alpha = 1$ if $h/d > 4$); f_{ck} – compressive strength of concrete cylinder (MPa); γ_v – safety sharing coefficient (generally 1.25).

In Table 11, experimental test in this paper, Lam's test, C1' and C11 specimens are selected and the shear resistance of the stud from the above specimens is compared to the calculation of standards ANSI/AISC-2005, ASSHTO-2012, CAN/CSA-16-01-2005 and EC4. It can be seen that each experimental result conforms to a different standard—the Lam's tests to CAN/CSA-16-01-2005, and the test in this paper to ANSI/AISC-2005. Moreover, FE model value of C1' fits well with 66.34 kN from

Table 11. Comparison of Test Value, FE Model Value and Theoretical Value

Specimens	Experimental value or FE model value (kN)	CAN theoretical value (kN)	ANSI theoretical value (kN)	AASHTO theoretical value (kN)	EC4 theoretical value (kN)
SP3	92.98	93.83	117.29	93.44	69.30
SP4	102.17	105.34	131.67	93.44	77.79
Test in this paper	66.50	53.07	66.34	46.45	42.46
C1’	66.49	53.07	66.34	46.45	42.46
C11	54.46	53.07	66.34	46.45	42.46

Note: SP3 and SP4 is controlled by the left term of the formula because of the low strength of concrete.

Table 12. Comparison between Simulated and Theoretical Value of Ultimate Stud Resistance

Specimen Code	AISC		AASHTO		CAN		EC4	
	$(V_2\text{-}V_u)/V_u$	$(V_2\text{-}V_l)/V_u$	$(V_2\text{-}V_u)/V_u$	$(V_2\text{-}V_l)/V_u$	$(V_2\text{-}V_u)/V_u$	$(V_2\text{-}V_l)/V_u$	$(V_2\text{-}V_u)/V_u$	$(V_2\text{-}V_l)/V_u$
C11	-17.86%	5.70%	17.37%	8.15%	2.56%	7.12%	28.14%	8.89%
C12	-19.55%	5.64%	14.92%	8.05%	0.56%	7.04%	25.64%	8.80%
C13	-21.51%	4.96%	12.13%	7.09%	-1.89%	6.20%	22.58%	7.75%
C14	-21.84%	5.38%	11.66%	7.68%	-2.29%	6.72%	22.07%	8.40%
AVG	-20.19%	5.42%	14.02%	7.74%	-0.27%	6.77%	24.61%	8.46%

Note: V_u = Ultimate shear resistance determined from relative specifications; V_1: Numerical analysis results without welding collar; V_2 : Numerical analysis results with welding collar.

ANSI/AISC-2005. While the C11 has the shear resistance of 54.46 kN, which fits with 53.07 kN from CAN/CSA-16-01-2005. In conclusion, the influence of welding collar on shear resistance of headed stud is included in the formulas of different specifications, but it is not separately reflected in the formula parameters. Therefore, when the dimension of welding collar is different, the test values may match with the different specification values.

In this paper, the influence of welding collar on shear resistance is separated, which is the basis of further study of the formula correction under different welding collar dimensions. Four groups of stud specimens in Group 3 are selected and their theoretical shear capacity is calculated respectively according to the above formula, as shown in Table 12. The results show that when C60 high-strength concrete is applied, the calculated value of formulas in various countries are controlled by the right term of the formula, which is because the C60 concrete adopted is high-strength concrete, the compressive strength value of the cylinder determines that the left term of the formula is greater than the right term of the formula. The shear resistance of the stud depends on its ultimate tensile strength.

With respect to the height-diameter ratio in this paper, the finite element calculation values of studs with different diameters approach the values obtained from the formula specified in CAN/CSA-S16-01.The average error between them is 1.83%, which shows that it is reasonable to quantify the dimension of welding collar by the height-diameter ratio. The contribution of welding collar to bearing capacity is about 6.77% of the CAN formula value, and the average value of bearing capacity of welding collar in various specification is 7.1%. In addition, the result of AISC formula is larger than that of finite element method, thus is inclined to be unsafe. The results of AASHTO formula are more conservative than the finite element results. The results of EC4 formula are the most conservative due to statistical analysis.

7. Conclusions

This paper investigates the influence of welding collar on the behavior of stud shear connector, the standard tests were conducted to confirm the accuracy of numerical analysis model and completed the theoretical research on the influence of several welding collar structural parameters on the shear behavior of stud . The major conclusions are as follows:

1. The comparison between the stud load-slip curve with consideration to the influence of the welding collar and the push-out test results indicates that the welding collar at the root of the stud can obviously improve the shear resistance of the headed stud.
2. The welding collar will affect the distribution of stud stress along the height direction, and the welding collar will increase the yield area at the bottom of the stud, thus dissipating more shear energy and further increasing the shear resistance of the headed stud.
3. The relationship between the relative volume ratio α of the welding collar and the percentage increase of the shear resistance of the stud is almost a linear. By analyzing the parameters of welding collar, the height of the welding collar has less effect on the shear resistance of the stud than the radius of the welding collar. The larger the radius of the welding collar with the same volume, the higher the efficiency of improving the shear resistance. Under the condition of

equal height-to-diameter ratio, shear resistance provided by the welding collar approximately converges to 7.28%, thus the increment range of shear resistance of studs with different diameters can be roughly estimated.

4. Compared with the classical formulas in various countries, AISC has a higher prediction value for the shear resistance of stud with high strength concrete, while the values of EC4 is the most conservative. Height-diameter ratio is a reasonable index to quantify the dimension of welding collar with different stud diameters. Under the condition of 0.25 height-diameter ratio, compared with predicted value of the CAN formula, the average relative error of shear resistance of studs with different diameters is only 1.83%. The shear resistance of welding collar is about 6.77% of the formula results. Since different dimensions of welding collar will cause errors, it is necessary to carry out further tests to correct the shear resistance of existing formulas under different dimensions of welding collar.
5. The results of this paper are only obtained on the basis of theoretical analysis. Multiple further experimental tests are needed to verify the correctness of the data.

Acknowledgments

This study was supported by the Sichuan Science and Technology Program (Grants, 2018GZ0052, and 2019YFH0139), the National Key Research and Development Program of China (Grant 2016YFB1200401) and the National Natural Science Foundation of China (Grants 51708466 and 51878564). And the Science and Technology Project of Ningbo Transportation Bureau is also gratefully acknowledged (Grant 202005).

Nomenclature

A_s = Cross-sectional area of stud
A_{st} = Cross-sectional area of stud
E_0 = Initial elastic modulus
f_c = Compressive strength of concrete cylinder
f_{ck} = Compressive strength of concrete cylinder
f_u = Ultimate tensile strength of stud
Q_d = Shear resistance of stud.
V_u = Shear resistance of stud
Vol_{-stud} = Volume of studs with the same height
Vol_{-ring} = Volume of welding collars with the same height.
α = Influence coefficient of stud length
α_1 = Influence parameter
γ_v = Safety sharing coefficient
ε_0 = Compressive strain
ε_u = Ultimate compressive strain
σ_0 = Peak stress
φ_{sc} = Bearing capacity coefficient

ORCID

Yulin Zhan https://orcid.org/0000-0002-4934-9989
Siji Lu https://orcid.org/0000-0002-2687-8124

References

AASHTO (2012) LRFD bridge design specifications. American Association of State Highway and Transportation Officials, Washington DC, USA, 154-161

ANSI/AISC 360-05 (2005) Specification for structural steel buildings. American National Standards Institute (ANSI)/AISC, Chicago, IL, USA, 80-87

ANSI/AWS C5.4-93 (1993) Recommended practices of stud welding, American National Standards Institute (ANSI)/AWS, Miami, FL, USA, 12-20

CAN/CSA-S16-01 (2005) Limit states design of steel structures. Canadian Standards Association, Toronto, Canada, 62-65

CECS226-2007 (2005) Technical specification for welding of stud. China Association for Engineering Construction Standardization, China Planning Press, Beijing, China (in Chinese)

Chambers HA (2001) Principles and practices of stud welding. *PCI Journal* 46(5):46-58, DOI: 10.15554/pcij.09012001.46.58

Chung CH, Lee J, Kim JS (2016) Shear strength of T-type Perfobond rib shear connectors. *KSCE Journal of Civil Engineering* 20(5):1824-1834, DOI: 10.1007/s12205-015-0095-8

Classen M, Herbrand M, Kueres D, Hegger J (2016) Derivation of design rules for innovative shear connectors in steel-concrete composites through the systematic use of non-linear finite element analysis (FEA). *Structural Concrrte* 17(4):646-655, DOI: 10.1002/suco.201500217

EC4 (2004) Design of composite steel and concrete structures. Part-1: General rules and rules for building (EC4). Brussels, Belgium, 54-60

EN ISO 13918 (2017) Welding — Studs and ceramic ferrules for arc stud welding. Irish Standard

GB50661-2011 (2011) Code for welding of steel structures. Ministry of Housing and Urban-Rural Development of the People's Republic of China, Beijing, China

Guezouli S, Lachal A (2012) Numerical analysis of frictional contact effects in push-out tests. *Engineering Structures* 40:39-50, DOI: 10.1016/j.engstruct.2012.02.025

Han Q, Wang Y, Xu J, Xing Y (2015) Static behavior of stud shear connectors in elastic concrete – Steel composite beams. *Journal of Constructional Steel Research* 113:115-126, DOI: 10.1016/j.jcsr.2015.06.006

Han Q, Wang Y, Xu J, Xing Y, Yang G (2017) Numerical analysis on shear stud in push-out test with crumb rubber concrete. *Journal of Constructional Steel Research* 130:148-158, DOI: 10.1016/j.jcsr.2016.12.008

Hanswille G, Porsch M, Ustundag C (2007) Resistance of headed studs subjected to fatigue loading: Part I: Experimental study. *Journal of Constructional Steel Research* 63(4):475-484, DOI: 10.1016/j.jcsr.2006.06.035

He S, Fang Z, Mosallam AS (2017) Push-out tests for perfobond strip connectors with UHPC grout in the joints of steel-concrete hybrid bridge girders. *Engineering Structures* 135:177-190, DOI: 10.1016/j.engstruct.2017.01.008

Higashiyama H, Yoshida K, Inamoto K, Matsui S, Kaido H (2014) Fatigue of headed studs welded with improved ferrules under rotating shear force. *Journal of Constructional Steel Research* 92:211-218,

DOI: 10.1016/j.jcsr.2013.09.012

Hildebrand J, Soltanzadeh H (2014) A review on assessment of fatigue strength in welded studs. *International Journal of Steel Structures* 14(2):421-438, DOI: 10.1007/s13296-014-2020-2

Hiragi H, Matsui S (1998) Investigation on remarkable improvement of fatigue strength for headed studs. *Proceedings of Developments in Short and Medium Span Bridge Engineering, Calgary* 16:81-93

Hirama, C, Ishikawa T, Hisagi A (2017) Shear strength of headed stud push-out tests: Comprehensive literature review focusing on slab type, failure mode, and large-diameter headed stud. *ce/papers* 1(2-3):2013-2022, DOI: 10.1002/cepa.246

Hognestad E (1951) Study of combined bending and axial load in reinforced concrete members. University of Illinois, Illinois, IL, USA, 43-54

Johnson RP, Greenwood RD, Dalen KV (1969) Stud shear-connectors in hogging moment regions of composite beams. *The Structural Engineer* 47(9):345-350

Lam D, El-Lobody E (2005) Behavior of headed stud shear connectors in composite beam. *Journal of Constructional Steel Research* 96:96-107, DOI: 10.1061/(ASCE)0733-9445(2005)131:1(96)

Luo Y, Hoki K, Hayashi K, Nakashima M (2016) Behavior and strength of headed stud–SFRCC shear connection. I: Experimental Study. *Journal of Structural Engineering* 142(2):04015112.1-04015112.10, DOI: 10.1061/(ASCE)ST.1943-541X.0001363

Ollgaard HG, Slutter RG (1971) Shear strength of stud connection in lightweight and normal-weight concrete. *Engineering Journal of American Institute of Steel Construction* 8(2):55-64

Pathirana SW, Uy B, Mirza O, Mirza O, Zhu X (2015) Strengthening of existing composite steel-concrete beams utilising bolted shear connectors and welded studs. *Journal of Constructional Steel Research* 114:417-30, DOI: 10.1016/j.jcsr.2015.09.006

Qi JN, Wang JQ, Li M, Chen L (2017) Shear capacity of stud shear connectors with initial damage: Experiment, FEM model and theoretical formulation. *Steel and Composite Structures* 25(1):79-92, DOI: 10.12989/scs.2017.25.1.079

Ranzi G, Bradford MA (2007) Composite beams with both longitudinal and transverse partial interaction subjected to elevated temperatures. *Engineering Structures* 29(10):2737-2750, DOI: 10.1016/j.engstruct.2007.01.022

Viest IM (1956) Investigation of stud shear connectors for composite concrete and steel T-beams. *ACI Journal* 27(8):875-981

Viest IM (1960) Review of research on composite steel-concrete beams. *Journal of Structural Division* 86(7):1-21

Wang J, Qi J, Tong T, Xu Q, Xiu H (2018) Static behavior of large stud shear connectors in steel-UHPC composite structures. *Engineering Structures* 178:534-542, DOI: 10.1016/j.engstruct.2018.07.058

Xu X, Liu Y, He J (2014a) Study on mechanical behavior of rubber-sleeved studs for steel and concrete composite structures. *Construction & Building Materials* 53:533-546, DOI: 10.1016/j.conbuildmat.2013.12.011

Xu C, Sugiura K, Masuya H, Hashimoto K, Fukada S (2014b) Experimental study on the biaxial loading effect on group stud shear connectors of steel-concrete composite bridges. *Journal of Bridge Engineering* 20(10):04014110, DOI: 10.1061/(ASCE)BE.1943-5592.0000718

Xue W, Ding M, Wang H (2008) Static behavior and theoretical model of stud shear connectors. *Journal of Bridge Engineering* 15(3):346-348, DOI: 10.1061/(ASCE)1084-0702(2008)13:6(623)